Universal Emergence of 1/*f* Noise in Asynchronously Tuned Elementary Cellular Automata

Daisuke Uragami
Department of Mathematical Information Engineering
College of Industrial Technology
Nihon University, Chiba, Japan
uragami.daisuke@nihon-u.ac.jp

Yukio-Pegio Gunji
Department of Intermedia Art and Science
School of Fundamental Science and Engineering
Waseda University, Tokyo, Japan
yukio@waseda.jp

In this paper, we propose asynchronously tuned elementary cellular automata (AT_ECA) as models that implement a new type of self-organized criticality (SOC). SOC in AT_ECA is based on asynchronously updating and locally tuning the consistency between dual modes of transition. A previous work showed that AT_ECA generate class 4-like spacetime patterns over a wide area of the rule space, and the density decay follows a power law for some of the rules. In this study, we performed a spectral analysis of AT_ECA, of which a great number of rules were found to exhibit $1/f$ noise, suggesting that AT_ECA realize critical states without selecting specific rules or fine-tuning parameters.

Keywords: cellular automata; $1/f$ noise; self-organizing criticality; asynchronous

1. Introduction

Various biological systems are found to be in critical states, but the mechanism of realizing such critical states is still unknown [1–4]. By a huge amount of analysis of one-dimensional cellular automata, Wolfram and Langton revealed that the critical states called class 4 exist only in the extremely narrow region of the rule space, which is the so-called edge of chaos [5, 6]. In recent years, Fatès and his colleagues have shown that asynchronous cellular automata have an asynchronous updating ratio as a parameter and the critical states are generated by tuning this parameter [7]. However, fine-tuning such parameters or rules in a real biological system is still a mystery.

https://doi.org/10.25088/ComplexSystems.27.4.399

Walker and his colleagues asserted that this is a serious problem, which modern science calls "the hard problem of life" [1].

Self-organizing criticality (SOC), which was proposed by Bak and his colleagues, is a candidate for solving this problem, in the sense that it realizes criticality without requiring the tuning of parameters [8, 9]. However, their models of SOC explicitly or implicitly include a mechanism for linking global and local information, and so they do not reveal all the mechanisms of SOC. In contrast, we have proposed another type of SOC based on thorough local interactions and coordination within the system [10–13]. In particular, asynchronously tuned elementary cellular automata (AT_ECA), as proposed by one of us, is a simple model that implements a new type of SOC and realizes criticality by asynchronous and nonuniform interactions. A previous study has found that AT_ECA generate class 4-like patterns over a wide area of the rule space, and the density decay follows the power law without fine-tuning the parameters [13, 14].

In this study, we analyzed the spacetime patterns of AT_ECA by calculating the power spectrum and found that $1/f$ noise is generated over a wide range of the rule space. $1/f$ noise can be found in many biological systems, but its universal mechanism is not yet clear [15]. On the other hand, since $1/f$ noise is often observed in criticality, it is a representative index for estimating whether a system is in a critical state [8]. Ninagawa reported that $1/f$ noise can be seen in spacetime patterns generated by a small number of rules, such as rule 110, in elementary cellular automata (ECA) [16]. Since these rules have computational universality [17], which is considered to be one of the features of biological systems, $1/f$ noise is considered to also be related to it [18]. In this study, the same analytical method that was used by Ninagawa for ECA was applied to AT_ECA. The results show that AT_ECA is a powerful model that offers a new picture of SOC in biological systems. The aim of this study is not to classify ECA or AT_ECA rules by $1/f$ noise. Our argument is that AT_ECA generates $1/f$ noise with many more rules compared to ECA. That argument is based on an analysis of the whole domain of rules.

2. Asynchronously Tuned Elementary Cellular Automata

AT_ECA introduce the following three factors to ECA, which are one-dimensional, two-state, three-neighbor cellular automata [13]:

1. Asynchronous updating.
2. Passive and active mode rules.
3. Tuning the active mode rule.

These three factors reveal local discrepancies and coordination between cells, which are involved in the one-step evolution. The local discrepancies and coordination are abandoned in the ECA, in which most of the features depend on synchronous updating [19, 20]. However, synchronous updating is not realistic in actual phenomena, such as biological systems. On the other hand, asynchronous updating may also be unrealistic, because it is attached to discrete modeling, but it is inevitable when using a mathematical model to describe phenomena. Such aspects of asynchronous updating are reflected in AT_ECA by the distinction among the passive mode, the active mode and the tuning rules. The discrepancy between the active and passive modes brought about by asynchronous updating is eliminated *ex post facto* by local coordination inside the system, which also inherits the next discrepancy [14].

The definition of AT_ECA, including the x at time step t:

$$x = 1, 2, \ldots, N, \tag{1}$$

$$t = 0, 1, \ldots, T - 1, \tag{2}$$

$$c_x(t) \in \{0, 1\}, \tag{3}$$

where N is the system size and T is the observation length of evolution. Asynchronous updating is introduced by an updating order, which is defined by

$$\mathrm{Ord}^t(x) \in \{1, 2, \ldots N\}, \tag{4}$$

$$x \neq y \Longrightarrow \mathrm{Ord}^t(x) \neq \mathrm{Ord}^t(y), \tag{5}$$

where $\mathrm{Ord}^t(x)$ is the order in which the value of site x is updated at time step t. $\mathrm{Ord}^t(x) = 1$ means that updating the value of site x is performed first, whereas $\mathrm{Ord}(x) = N$ means that updating is performed last. $\mathrm{Ord}^t(x)$ is randomly determined, but without duplication for each time step. In other words, $\mathrm{Ord}^t(x)$ is a one-to-one and onto map.

There are two modes of local rules used for updating the value of each site: passive and active. The passive mode rule ϕ^P is a function that is defined as follows:

$$\phi^P : \{0, 1\}^3 \to \{0, 1\}, \tag{6}$$

$$\frac{111}{d_7}\ \frac{110}{d_6}\ \frac{101}{d_5}\ \frac{100}{d_4}\ \frac{011}{d_3}\ \frac{010}{d_2}\ \frac{001}{d_1}\ \frac{000}{d_0}, \tag{7}$$

https://doi.org/10.25088/ComplexSystems.27.4.399

$$d_s \in \{0, 1\}\ (s = 0, 1, \ldots, 7). \tag{8}$$

In equation (7), the three-bit number above the line is an input of ϕ^P, whereas d_s is the corresponding output; that is, $\phi^P(0, 0, 0) = d_0$, $\phi^P(0, 0, 1) = d_1, \ldots, \phi^P(1, 1, 1) = d_7$. By specifying d_s for all $0, 1, \ldots, 7$, a passive mode rule is specifically determined. There are $2^8 = 256$ combinations of d_s, which are consistent with the local rules of ECA. The rules are denoted by Wolfram's rule number from 0 to 255 [21]. Likewise, AT_ECA are assigned a number from 0 to 255 according to the passive mode rule, which is invariant among all sites and through all time steps. On the other hand, the active mode rule differs at each site and varies with the time steps. The active mode rule $\phi^A_{x,t}$ of site x at time step t is defined by

$$\phi^A_{x,t} : \{0, 1\}^3 \to \{0, 1\}, \tag{9}$$

$$\frac{111}{e^t_{7,x}}\ \frac{110}{e^t_{6,x}}\ \frac{101}{e^t_{5,x}}\ \frac{100}{e^t_{4,x}}\ \frac{011}{e^t_{3,x}}\ \frac{010}{e^t_{2,x}}\ \frac{001}{e^t_{1,x}}\ \frac{000}{e^t_{0,x}}, \tag{10}$$

$$e^t_{s,x} \in \{0, 1\}\ (s = 0, 1, \ldots, 7). \tag{11}$$

Similarly to equation (7), the upper and lower sides of the line of equation (10) represent the input of function $\phi^A_{x,t}$ and the corresponding output, respectively; that is,

$$\phi^A_{x,t}(0, 0, 0) = e^t_{0,x},$$
$$\phi^A_{x,t}(0, 0, 1) = e^t_{1,x}, \ldots, \phi^A_{x,t}(1, 1, 1) = e^t_{7,x}.$$

Using the passive mode rule, the active mode rule and an updating order, the value of each site is updated according to the following:

$$\mathrm{Ord}^t(x-1) < \mathrm{Ord}^t(x) < \mathrm{Ord}^t(x+1) \Longrightarrow c_x(t+1) = \phi^P(c_{x-1}(t+1), c_x(t), c_{x+1}(t)), \tag{12a}$$

$$\mathrm{Ord}^t(x-1) > \mathrm{Ord}^t(x) > \mathrm{Ord}^t(x+1) \Longrightarrow c_x(t+1) = \phi^P(c_{x-1}(t), c_x(t), c_{x+1}(t+1)), \tag{12b}$$

$$\mathrm{Ord}^t(x-1) < \mathrm{Ord}^t(x) > \mathrm{Ord}^t(x+1) \Longrightarrow c_x(t+1) = \phi^P(c_{x-1}(t+1), c_x(t), c_{x+1}(t+1)), \tag{12c}$$

$$\mathrm{Ord}^t(x-1) > \mathrm{Ord}^t(x) < \mathrm{Ord}^t(x+1) \Longrightarrow c_x(t+1) = \phi^A_{x,t}(c_{x-1}(t), c_x(t), c_{x+1}(t)). \tag{12d}$$

These four equations are for calculating $c_x(t+1)$, which is the value of site x at time step $t+1$, and are conditioned according to the updating order of site x and the neighboring sites. Equations (12a)–(12c) are applied in the case where one or two sites that have already

been updated are included in the neighboring sites. In this case, $c_x(t+1)$ is calculated by referring to $c_{x-1}(t+1)$ and/or $c_{x+1}(t+1)$, which are the values at time step $t+1$. Equation (12d) is applied in the case where an updated site is not included in the neighboring sites. In this case, $c_x(t+1)$ is calculated by referring to the values only at time step t. Note that equations (12a)–(12c) include the passive mode rule ϕ^P and equation (12d) includes the active mode rule $\phi^A_{x,t}$; that is, the value of a site at the next time step is calculated using the passive mode rule if the neighbor includes the updated site; otherwise, the active mode rule is used.

Now, we explain the tuning rule. At the beginning of the evolution, the active mode rule is the same as the passive mode rule. So,

$$e^0_{s,x} = d_s \ (s = 0,\ 1, \ldots, 7). \tag{13}$$

The active mode rule is tuned by determining $e^{t+1}_{s,x}$ as follows:

$$\text{for } m = 4 \cdot c_{x-1}(t) + 2 \cdot c_x(t) + c_{x+1}(t),$$

$$\text{Ord}^t(x-1) < \text{Ord}^t(x) < \text{Ord}^t(x+1) \Longrightarrow e^{t+1}_{m,x} = d_0, \tag{14a}$$

$$\text{Ord}^t(x-1) > \text{Ord}^t(x) > \text{Ord}^t(x+1) \Longrightarrow e^{t+1}_{m,x} = d_0, \tag{14b}$$

$$\text{Ord}^t(x-1) < \text{Ord}^t(x) > \text{Ord}^t(x+1) \Longrightarrow e^{t+1}_{m,x} = c_x(t+1), \tag{14c}$$

$$\text{Ord}^t(x-1) > \text{Ord}^t(x) < \text{Ord}^t(x+1) \Longrightarrow e^{t+1}_{m,x} = e^t_{s,x}. \tag{14d}$$

Equations (14a)–(14c) represent the case when the passive mode rule is applied to calculate $c_x(t+1)$, in which case the active mode rule is changed. d_0 in equations (14a) and (14b) is included in equation (7). When only one of the neighboring sites is updated before the center sites, the corresponding output of the active mode rule is canceled, so as to coincide with the output corresponding to input $(0, 0, 0)$ in the passive mode rule. Equation (14c) represents the case when both neighboring sites are updated before the center site, in which case the corresponding output of the active mode rule is changed to coincide with $c_x(t+1)$. Equation (14c) is the most essential for the updating of the active mode rule. By tuning the active rule in this way, the discrepancy between the passive and the active modes is adjusted to become small. Equation (14d) represents the case when the active mode rule is applied to calculate $c_x(t+1)$, in which case the active mode rule is not changed. Also, the outputs of the active mode rule corresponding to inputs other than m are not changed. So,

$$e^{t+1}_{s,x} = e^t_{s,x} \ (s \neq m). \tag{15}$$

https://doi.org/10.25088/ComplexSystems.27.4.399

3. Universal Emergence of 1/*f* Noise

Power spectra are calculated for the spacetime patterns generated by AT_ECA. The calculation method is the same as that Ninagawa applied to ECA [16, 18, 22]. A spacetime pattern is a set of the site values $c_x(t)(x = 1, 2, \ldots, N, t = 0, 1, \ldots, T-1)$. The power spectrum of a spacetime pattern is calculated as follows:

$$\hat{c}_x(f) = \frac{1}{T}\sum_{t=0}^{T-1} c_x(t)\ \exp\left(-i\frac{2\pi tf}{T}\right), \quad f = 0, 1, \ldots, T-1, \tag{16}$$

$$S(f) = \sum_{x=1}^{N} |\hat{c}_x(f)|^2. \tag{17}$$

Equation (16) gives the discrete Fourier transform for a time series of values of site x for $t = 0, 1, \ldots, T-1$, where f is the frequency that corresponds to the period T/f. The summation of the squared absolute values of the frequency component $\hat{c}_x(f)$ for all sites gives the power $S(f)$. The power intuitively means the strength of the periodic vibration with period T/f in the spacetime pattern. We use random initial conditions and a periodic boundary condition.

First, we describe the results of the analysis of a typical case. Figure 1 shows the spacetime patterns and the power spectra of rule 60 in AT_ECA and ECA. The spacetime patterns consist of 200 sites for 200 time steps. The power spectra are calculated from the evolution of 200 sites for 1024 time steps and are indicated by double logarithms. The spacetime pattern of the ECA is chaotic and typically classified as class 3 according to Wolfram's classification. The power spectrum of the ECA is uniformly distributed with respect to the frequency, which is the so-called white noise. On the other hand, the spacetime pattern of the AT_ECA shows that some local patterns grow like a branch. This pattern is typically classified as class 4 according to Wolfram's classification. The power spectrum of the AT_ECA is distributed in a negative slope with respect to frequency, indicating the so-called $1/f$ noise. The broken line represents the least-squares fitting of the power spectrum. The slope α and the residual sum of squares σ^2 are calculated using the following equations:

$$\log(S(f)) = -\alpha\cdot\log(f) + \beta, \tag{18}$$

$$\sigma^2 = \frac{1}{f_r}\sum_{f=1}^{f_r}\left(\log(S(f)) - \left(-\alpha\cdot\log(f) + \beta\right)\right)^2, \tag{19}$$

where $f_r = 100$, so the fitting is performed in the range of $f = 1 \sim 100$. As a result, the slope is $\alpha = 1.001$ and the residual sum

of squares is $\sigma^2 = 0.0033$. The slope is close to 1 and can be said to fit well. To confirm the reproducibility of this result, Figure 2 plots the slope on the horizontal axis and the residual sum of squares on the vertical axis for 100 trials, starting from a random initial configuration. The 95% confidence interval of the population mean of the slope is $\langle \alpha \rangle = 1.0096 \pm 0.0042$.

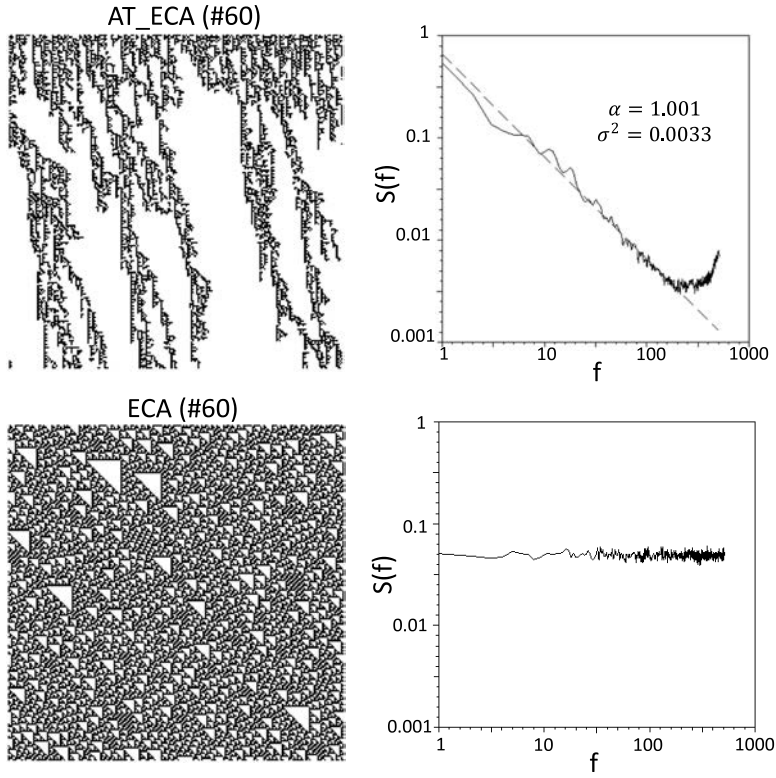

Figure 1. Spacetime patterns (left) and power spectra (right) of AT_ECA rule 60 (top) and ECA rule 60 (bottom). The power spectra are plotted on a log–log scale. The broken line in the power spectrum represents the least-squares fitting of the power spectrum in the range $f = 1 \sim 100$ with slope $\alpha = 1.001$ and residual sum of squares $\sigma^2 = 0.0033$.

Next, we show by exhaustive analysis that $1/f$ noise is universally generated for the rule space in AT_ECA. Figure 3 plots the slopes of the power spectra and the residual sum of squares for all 256 rules. Each point is an average value of 10 trials. The left plot is related to AT_ECA and the right plot is related to ECA. In AT_ECA, there are more points located at the lower right of the graph than in ECA. In other words, AT_ECA include more rules with a larger slope and a

smaller residual sum of squares, which is less than ECA rules 54, 62 and 110, which are known to exhibit power spectra close to $1/f$ noise. Thus, it can be concluded that $1/f$ noise is generated by these rules in AT_ECA. It should be noted that although many ECA rules exist outside the plot range, the power spectra clearly differ from $1/f$ noise (the residual sum of squares is very large or the slope is smaller than 0).

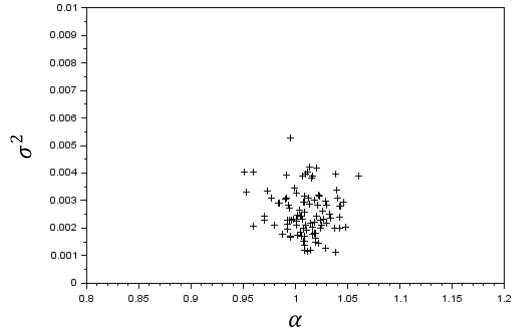

Figure 2. The residual sum of squares σ^2 versus the slope α of the least-squares fitting of the power spectrum for 100 runs by AT_ECA rule 60.

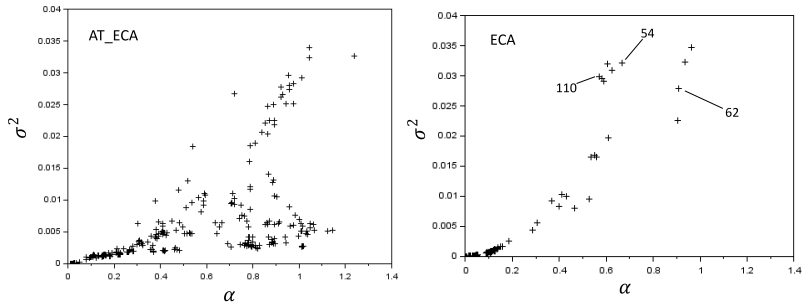

Figure 3. The residual sum of squares σ^2 versus the slope α of the least-squares fitting of the power spectrum for all rules of AT_ECA (left) and ECA (right). Each cross represents the average of 10 runs for each rule.

Table 1 lists the rule numbers whose slope is greater than 0.5 and whose residual sum of squares is less than 0.5 in the results of the analysis of AT_ECA, as shown in Figure 3. The rule numbers included in parentheses generate the same spacetime patterns by the symmetry of rules in ECA [23]. Due to the equations (14a) and (14b) in the tuning rule, the symmetry of 0 and 1 is broken in AT_ECA. However, left and right symmetry is kept in AT_ECA. Therefore, in AT_ECA, rules 166 and 180 are equivalent. Rule 188 and rule 230

6 (159 20 215)	14 (143 84 213)	22 (151)
38 (155 52 211)	46 (139 116 209)	54 (147)
60 (195 102 153)	88	90 (165)
110 (137 124 193)	134 (148)	142(212)
150	156	161
166 (180)	174 (244 208)	182
188 (230)	218	242
250		

Table 1. Numbers represent rules of AT_ECA whose slopes are greater than 0.5 and whose residual sums of squares are less than 0.005. Rules included in parentheses are equivalent in ECA under the symmetries 0/1 and left/right.

are also equivalent. On the other hand, rule 160 and rule 250 are not equivalent. Forty-nine rules of AT_ECA are included in this table, but ECA does not have any rules that satisfy this condition. For nine rules out of those described in Table 1, the spacetime patterns and the power spectra are shown in Figures 4–6. For comparison, the spacetime pattern and the power spectrum of ECA with the same rule number are also displayed. These nine rules consist of various rules

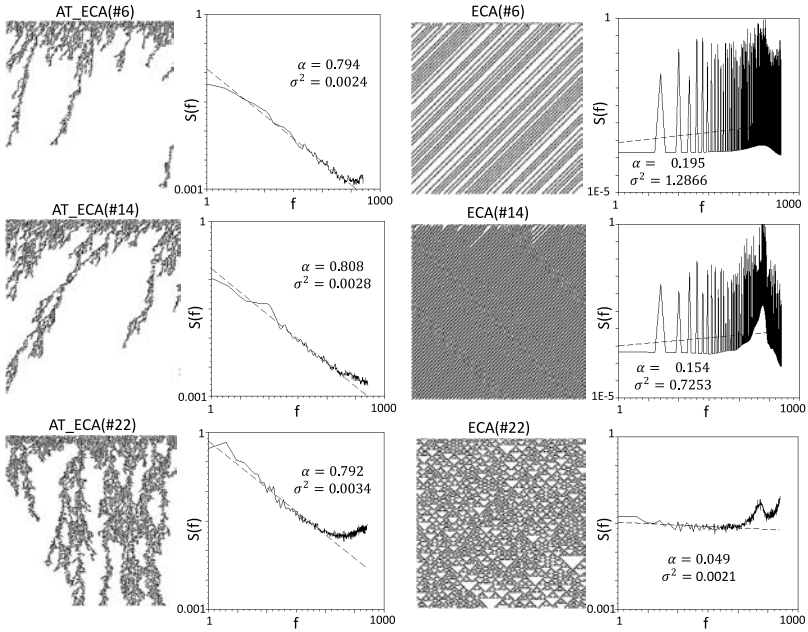

Figure 4. Spacetime patterns and power spectra of AT_ECA (left) and ECA (right) with rule 6 (top), rule 14 (middle) and rule 22 (bottom). The power spectra are plotted on a log–log scale. The broken line in the power spectrum represents the least-squares fitting of the power spectrum in the range $f = 1 \sim 100$ with slope α and residual sum of squares σ^2.

whose spacetime patterns in ECA are periodic (6 and 14), chaotic (22 and 110), critical (54 and 110) and fixed (156, 218, and 250). It can be confirmed that all these rules generate $1/f$ noise in AT_ECA. The analysis clarified that $1/f$ noise is universally generated for various rules in AT_ECA.

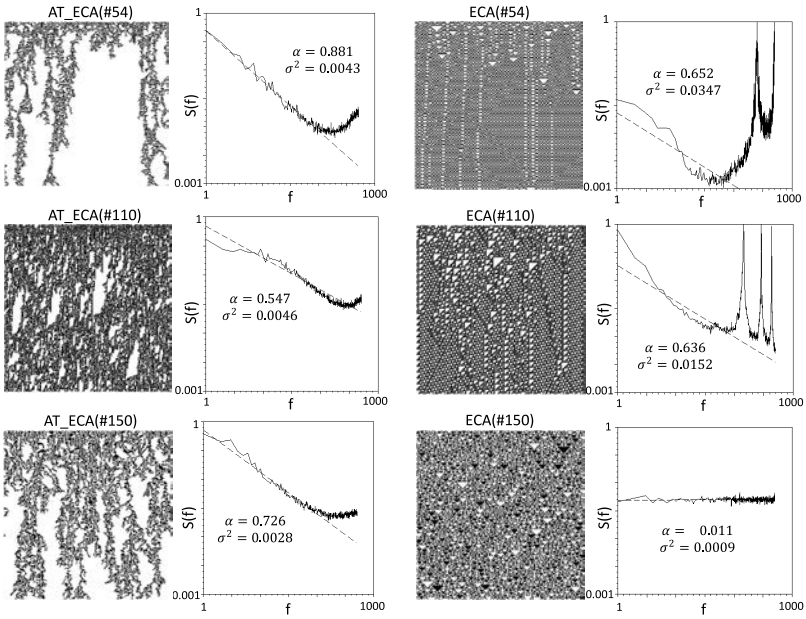

Figure 5. Spacetime patterns and power spectra of AT_ECA (left) and ECA (right) with rule 54 (top), rule 110 (middle) and rule 150 (bottom).

To investigate the factors that generate $1/f$ noise in AT_ECA, the same analysis is performed for asynchronous elementary cellular automata (A_ECA), which introduces only asynchronous updating into ECA. Figure 7 shows the spacetime pattern and the power spectrum for A_ECA rule 60. The simulation conditions are the same as those shown in Figure 1. The spacetime pattern is more chaotic than that of AT_ECA. The power gradually decreases in the high-frequency region and shows a property close to $1/f$ noise, but in the low-frequency region, the power is almost constant and shows white noise. Figure 8 shows the slope of the power spectrum and the residual sum of squares for all rules in A_ECA. The conditions of analysis are the same as those shown in Figure 3. Comparing Figure 8 with Figure 3, we can see that the distribution of A_ECA is similar to that of ECA but different from that of AT_ECA. In A_ECA, there is no point located at the lower right of the graph; that is, there is no rule

in which the slope is large and the residual sum of squares is small. Therefore, there is no rule indicating $1/f$ noise in A_ECA. We can conclude that $1/f$ noise does not occur only with asynchronous updating and that locally tuning the consistency between the passive and the active modes together with asynchronous updating generates $1/f$ noise in AT_ECA.

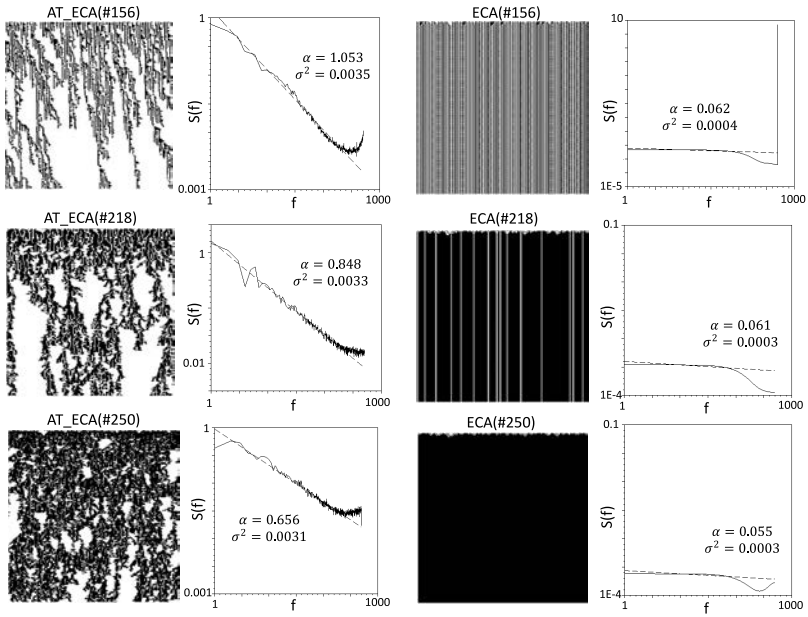

Figure 6. Spacetime patterns and power spectra of AT_ECA (left) and ECA (right) with rule 156 (top), rule 218 (middle) and rule 250 (bottom).

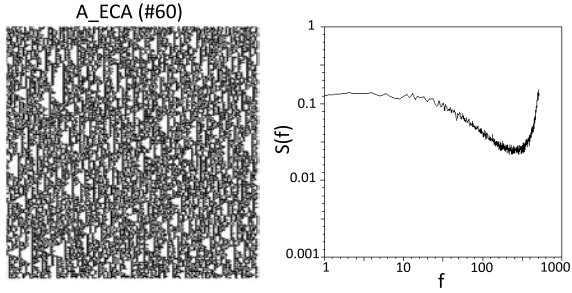

Figure 7. Spacetime patterns (left) and power spectra (right) of A_ECA rule 60.

https://doi.org/10.25088/ComplexSystems.27.4.399

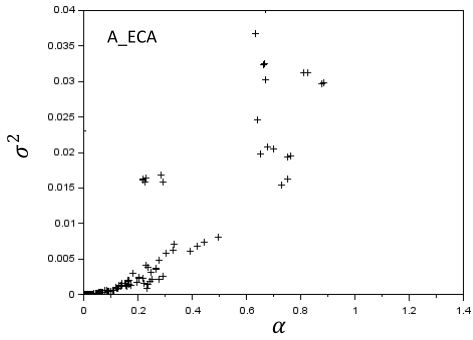

Figure 8. The residual sum of squares σ^2 versus the slope α of the least-squares fitting of the power spectrum for all rules of A_ECA.

4. Independence of the System Size and Observation Length

We investigated the dependence of the power spectrum on the system size and observation length. In general, when the observation length is too long as compared with the system size, the slope of the power spectrum becomes small in the low-frequency region and it is not the $1/f$ noise. The reason for this is considered to be the observation length being large relative to the system size, the growth of the branch pattern being interrupted and the configuration becoming uniform. However, it is known that there are some rules in AT_ECA of which the densities (the ratio of sites with the value 1) decrease according to the power law with respect to the time steps [13]. Regarding these rules, it can be expected that the power spectrum maintains the $1/f$ noise type even if the observation length is very large. So, regarding rule 150, the dependence on the observation length is examined in detail. Figure 9 plots the slope of the power spectrum for observation lengths $T = 1000$, 2000, 3000, 4000, 5000, 6000, 7000, 8000, 9000 and 10 000. Each point is the average value of 30 trials. The upper plot in Figure 9 shows the slopes of the least-squares fitting of the spectra from $f = 1$ to 100. In the case of system size $N = 100$, the slope tends to rise slightly as the observation length is increased, but it is nearly constant from $T = 4000$ to 9000. In the case of system size $N = 1000$, the slope is almost constant from $T = 2000$.

The lower part of Figure 9 shows the slope of the least-squares fitting of the power spectrum from $f = 1$ to 10. It focuses on the low-frequency region where the dependence on the observation length is expected to be larger. AT_ECA rule 150 and ECA rule 110 are displayed with system size $N = 100$. ECA rule 110 is known to exhibit $1/f$ noise during the longest time steps in this frequency range [16].

However, according to the graph, the slope of ECA rule 110 decreases as the time size increases, because periodical spacetime patterns are generated because of the small system size. On the other hand, the slope of AT_ECA rule 150 slightly tends to increase as the time size increases, but the slope is within the range of 0.8–1.1. These results indicate that AT_ECA generates $1/f$ noise in the long-period frequency region even though the system size is small.

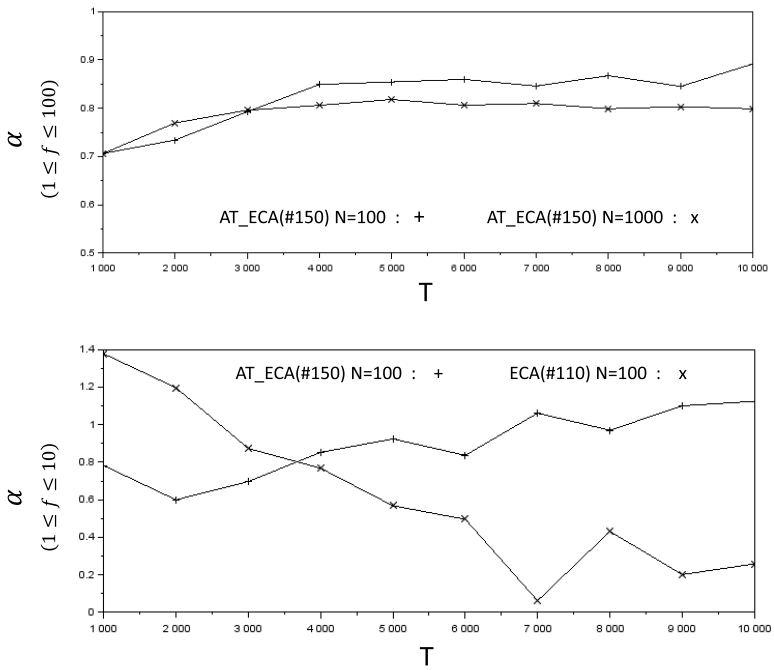

Figure 9. Average slope of power spectra for 30 runs versus time size. The least-squares fitting of the power spectrum is performed in the range $f = 1 \sim 100$ (top) and $f = 1 \sim 10$ (bottom). In the top graph, "+" represents AT_ECA rule 150 with $N = 100$ and "x" represents AT_ECA rule 150 with $N = 1000$. In the bottom graph, "+" represents AT_ECA rule 150 with $N = 100$ and "x" represents ECA rule 110 with $N = 100$.

This result can clearly be seen from the power spectrum shown in Figure 10. Each is the average power spectrum of 30 trials, which are part of the results of the analysis shown in Figure 9. Regarding AT_ECA rule 150, even if the system size is smaller or the observation length is larger, the shape of the power spectrum hardly changes but shows $1/f$ noise (Figure 10, left and center). On the other hand, in the case of ECA rule 110, when the system size is small and the

observation length is large ($N = 100$, $T = 10\,000$), the power spectrum is clearly different from $1/f$ noise (Figure 10, lower right). Summarizing the results, it can be said that AT_ECA rule 150 universally generates $1/f$ noise without depending on the space size and observation length.

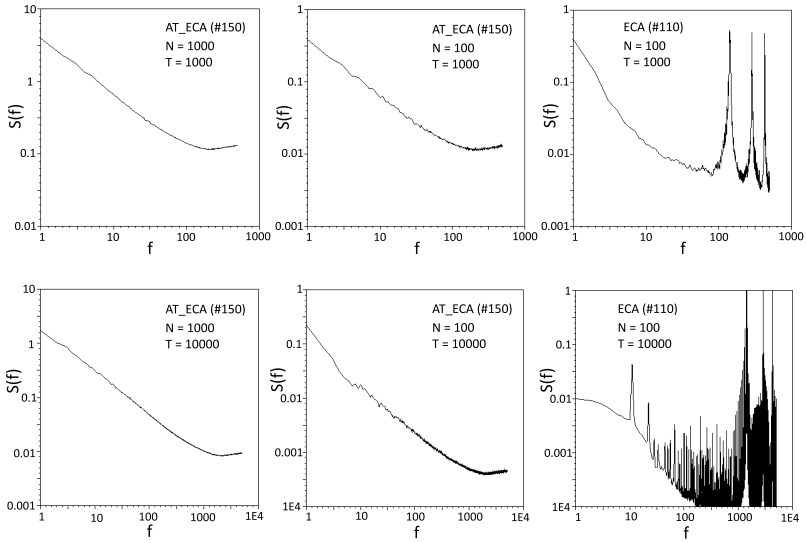

Figure 10. Average power spectra for 30 runs of AT_ECA rule 150 with $N = 1000$ and $T = 1000$ (top left), $N = 1000$ and $T = 10\,000$ (bottom left), $N = 100$ and $T = 1000$ (top center), and $N = 100$ and $T = 10\,000$ (bottom center); and ECA rule 110 with $N = 100$ and $T = 1000$ (top right), and $N = 100$ and $T = 10\,000$ (bottom right).

5. Conclusion

In this study, we calculated the power spectra of the spacetime patterns generated by asynchronously tuned elementary cellular automata (AT_ECA) and revealed that AT_ECA exhibit $1/f$ noise in a very large number of rules. We also found that certain rules exhibit $1/f$ noise during very long time steps, regardless of the system size. We can conclude that AT_ECA realizes the criticality without a fine selection of rules and fine-tuning parameters, such as spacetime size, since $1/f$ noise is a representative index of criticality. Furthermore, AT_ECA does not have global information as other self-organizing criticality (SOC) models do. Therefore, AT_ECA present a new picture of SOC, which is realized by perpetual inconsistency and local coordination within the system.

References

[1] S. I. Walker and P. C. W. Davies, "The "Hard Problem" of Life," in *From Matter to Life: Information and Causality* (S. I. Walker, P. C. W. Davies and G. F. R. Ellis, eds.), New York: Cambridge University Press, 2017 pp. 19–37.

[2] S. A. Kauffman, "Metabolic Stability and Epigenesis in Randomly Constructed Genetic Nets," *Journal of Theoretical Biology*, **22**(3), 1969 pp. 437–467. doi:10.1016/0022-5193(69)90015-0.

[3] D. R. Chialvo and P. Bak, "Learning from Mistakes," *Neuroscience*, **90**(4), 1999 pp. 1137–1148. doi:10.1016/S0306-4522(98)00472-2.

[4] T. Rohlf, N. Gulbahce and C. Teuscher, "Damage Spreading and Criticality in Finite Random Dynamical Networks," *Physical Review Letters*, **99**(24), 2007 248701. doi:10.1103/PhysRevLett.99.248701.

[5] S. Wolfram, "Universality and Complexity in Cellular Automata," *Physica D: Nonlinear Phenomena*, **10**(1–2), 1984 pp. 1–35. doi:10.1016/0167-2789(84)90245-8.

[6] C. G. Langton, "Computation at the Edge of Chaos: Phase Transitions and Emergent Computation," *Physica D: Nonlinear Phenomena*, **42**(1–3), 1990 pp. 12–37. doi:10.1016/0167-2789(90)90064-V.

[7] N. Fatès, "Asynchronism Induces Second Order Phase Transitions in Elementary Cellular Automata," *Journal of Cellular Automata*, **4**(1), 2009 pp. 39–54.

[8] P. Bak, C. Tang and K. Wiesenfeld, "Self-Organized Criticality: An Explanation of the $1/f$ Noise," *Physical Review Letters*, **59**(4), 1987 pp. 381–384. doi:10.1103/PhysRevLett.59.381.

[9] P. Bak and K. Sneppen, "Punctuated Equilibrium and Criticality in a Simple Model of Evolution," *Physical Review Letters*, **71**(24), 1993 pp. 4083–4086. doi:10.1103/PhysRevLett.71.4083.

[10] K. Ito and Y.-P. Gunji, "Self-Organization toward Criticality in the Game of Life," *Biosystems*, **26**(3), 1992 pp. 135–138. doi:10.1016/0303-2647(92)90072-7.

[11] Y.-P. Gunji and M. Kamiura, "Observational Heterarchy Enhancing Active Coupling," *Physica D: Nonlinear Phenomena*, **198**(1–2), 2004 pp. 74–105. doi:10.1016/j.physd.2004.08.021.

[12] D. Uragami and Y.-P. Gunji, "Lattice-Driven Cellular Automata Implementing Local Semantics," *Physica D: Nonlinear Phenomena*, **237**(2), 2008 pp. 187–197. doi:10.1016/j.physd.2007.08.010.

[13] Y.-P. Gunji, "Self-Organized Criticality in Asynchronously Tuned Elementary Cellular Automata," *Complex Systems*, **23**(1), 2014 pp. 55–69. complex-systems.com/pdf/23-1-3.pdf.

[14] Y.-P. Gunji, "Extended Self Organised Criticality in Asynchronously Tuned Cellular Automata," *Chaos, Information Processing and Paradoxical Games: The Legacy of John S. Nicolis* (G. Nicolis and V. Basios, eds.), Hackensack, NJ: World Scientific, 2015 pp. 411–429. doi:10.1142/9789814602136_ 0021.

[15] L. M. Ward and P. E. Greenwood, "$1/f$ Noise," *Scholarpedia*, **2**(12), 2007 1537. doi:10.4249/scholarpedia.1537.

[16] S. Ninagawa, "Power Spectral Analysis of Elementary Cellular Automata," *Complex Systems*, **17**(4), 2008 pp. 399–411. complex-systems.com/pdf/17-4-5.pdf.

[17] M. Cook, "Universality in Elementary Cellular Automata," *Complex Systems*, **15**(1), 2004 pp. 1–40. complex-systems.com/pdf/15-1-1.pdf.

[18] S. Ninagawa, "Dynamics of Universal Computation and $1/f$ Noise in Elementary Cellular Automata," *Chaos, Solitons & Fractals*, **70**, 2015 pp. 42–48. doi:10.1016/j.chaos.2014.11.001.

[19] T. E. Ingerson and R. L. Buvel, "Structure in Asynchronous Cellular Automata," *Physica D: Nonlinear Phenomena*, **10**(1–2), 1984 pp. 59–68. doi:10.1016/0167-2789(84)90249-5.

[20] N. A. Fatès and M. Morvan, "An Experimental Study of Robustness to Asynchronism for Elementary Cellular Automata," *Complex Systems*, **16**(1), 2005 pp. 1–27. complex-systems.com/pdf/16-1-1.pdf.

[21] S. Wolfram, "Statistical Mechanics of Cellular Automata," *Reviews of Modern Physics*, **55**(3), 1983 pp. 601–644. doi:10.1103/RevModPhys.55.601.

[22] K. Nakajima and T. Haruna, "Self-Organized Perturbations Enhance Class IV Behavior and $1/f$ Power Spectrum in Elementary Cellular Automata," *BioSystems*, **105**(3), 2011 pp. 216–224. doi:10.1016/j.biosystems.2011.05.002.

[23] W. Li and N. Packard, "The Structure of the Elementary Cellular Automata Rule Space," *Complex Systems*, **4**(3), 1990 pp. 281–297. complex-systems.com/pdf/04-3-3.pdf.